IEEE Access
Multidisciplinary : Rapid Review : Open Access Journal

Received August 31, 2019, accepted September 10, 2019, date of publication September 18, 2019, date of current version October 1, 2019.

Digital Object Identifier 10.1109/ACCESS.2019.2942200

Modeling and Optimization for Connection Design of the Asymmetric-Paths Winding by Novel Combinatorial Approach

YANPING LIANG, ZHONGQI GUO, XU BIAN, CHENGUANG WANG, DONGMEI WANG, AND LIANLIAN GAO
College of Electrical and Electronic Engineering, Harbin University of Science and Technology, Harbin 150080, China

Corresponding author: Yanping Liang (liangyanping2010@126.com)

This work was supported in part by the National Natural Science Foundation of China under Grant 51807040, in part by the Natural Science Foundation of Heilongjiang Province under Grant ZD2019E008, and in part by the National Natural Science Foundation of China under Grant 51477038.

ABSTRACT This paper proposes a novel combinatorial approach for the optimization design of the asymmetric-paths winding, to solve the design contradiction between the asymmetric degree and the tidiness of end connections. In the proposed approach, the combinatorial models for the arrangement and the connection are built. In addition, some grouping strategies are applied into the combinatorial models, and some matching strategies are provided to deal with the combination of coils among groups for the optimized arrangement. At last, the winding design of a large hydro-generator combing with the electromagnetic analysis is provide for the validation. The results show that the optimized design presents a low asymmetric degree between parallel paths as well as a tidy connection of end windings simultaneously, which are better than the existing designs. This approach provides a novel idea for the modeling and optimization design for the ac windings, especially for the asymmetric-paths windings.

INDEX TERMS Asymmetric-paths winding, combinatorial approach, connection optimization, winding design, AC machines.

I. INTRODUCTION

It is well known that the performance and cost are the ultimate design goal in electric machines [1], [2], which are mostly depended on the design of stator windings. The asymmetric-paths winding is a novel ac winding with a fractional ratio for the number of poles to the number of parallel paths, which provides more flexible choice for the number of parallel paths [3]–[5]. It is very suitable for the economy improvement of large machines, and has been implemented into some designs [6], [7]. This technology presents a wide development potential.

In view of the asymmetrical distribution of path windings, the difference of the resulting electromotive force (EMF) between parallel paths could be caused, which will result in the circulating current between parallel paths and the increase of the winding losses. The asymmetric degree can be reduced by adjusting the combination of slot-vectors of parallel paths [8]. But it has rarely encountered in the general designs, which mainly focus on the asymmetrical distributions of phase windings [9]–[11]. In addition, the tidiness of end connections for the some unusual arrangements with a small asymmetric degree can be not ensured, owing to the complex distributions of coils. Thus, the cost and fixation difficulty of windings will rise. The optimization method based on the directed graph is proposed in [12]. But the searching number could increase obviously for the cases of multiple numbers of slots and parallel paths. With respect to the existing research, these studies mainly focus on the combination of coils rather than the connected relationship between coils, such as the different connection types of winding terminals [13]–[15] and the different connection schemes of phase change [16], [17]. To sum up, the design contradiction between the asymmetric degree between parallel paths and the tidiness of end connections is still pending to be solved.

The associate editor coordinating the review of this manuscript and approving it for publication was Xiaodong Sun.

With respect to general designs, some strategies are adopted to improve the performance, such as different structures, dimensional changes, and different slot-pole combinations [18]–[22]. According to the design feature of windings, in practical, the optimization for the length of the connected wires can be regarded as a kind of the combination optimization like the shortest path in traveling salesman problems [23], [24]. It presents an effective potential to solve most engineering problems [25]–[27]. With respect to the similar studies, they mainly adopt the optimization algorithms to solve the modeling on the structure of machines [28]–[30]. The application on the connection of windings has yet to be developed.

In this paper, a novel combinatorial approach is proposed to deal with the design contradiction above. The structure of paper is arranged as follows: In section II, basis design features and constraints for the asymmetric-paths winding are introduced. In section III, main procedures of strategies and rules of operations for the proposed approach are provided particularly. In section IV, the comparisons of the designs of a hydro-generator combining with the electro-magnetic analysis are presented for the validation.

II. DESIGN CHARACTERISTICS

A. PARAMETER CONSTRAINTS

The configuration of the stator winding is shown in Fig. 1. With respect to the asymmetric-paths winding, on one hand, the ratio for the number of poles to the number of parallel paths should be fractional. On the other hand, the total number of slot-vectors for each parallel path should be the same to ensure the symmetrical distribution between phase windings and the maximum output voltage. Hence, the winding parameters should be followed as:

$$\begin{cases} \dfrac{2p}{a} \neq \text{int} \\ n_1 = \dfrac{Z}{m \times a} = \text{int} \end{cases} \tag{1}$$

where p is the number of pole-pairs, a is the number of parallel paths, n_1 is the number of slots per parallel path, Z is the number of slots, and m is the number of phases.

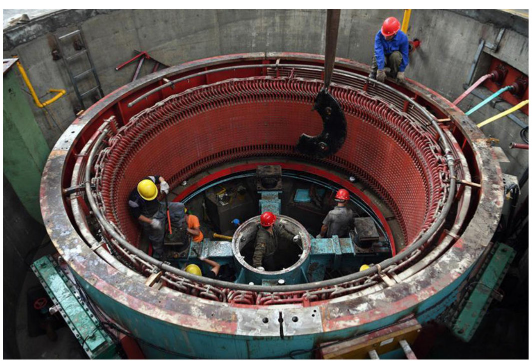

FIGURE 1. Configuration for the stator winding of a large machine.

B. ARRANGEMENT

The arrangement of the asymmetric-paths winding can be regarded as the assignment of slot-vectors for each parallel path from the square graph. The square graph is a square table of coils, and it can be expressed as:

$$\mathbf{N} = \left[n_{i,j}\right]_{p \times q} \tag{2}$$

where $n_{j,k}$ is the element of the square graph in a phase-belt, it represents a coil numbered by the slot number of the upper side, j is the row number, k is the column number, and q is the number of slots per pole per phase.

In this paper, because of the same distribution of windings in phase-belt A and X, only consider the distribution of windings in phase-belt A is enough. Corresponding coil number can be calculated by:

$$n_{j,k} = 2m \cdot q \cdot (j-1) + k \tag{3}$$

The arrangement can be expressed in a form of the path slot-number matrix, and it can be defined as:

$$\mathbf{B} = \left[b_{j,k}\right]_{(a/2) \times q} \tag{4}$$

where $b_{j,k}$ is the element of the path slot-number matrix, it represents the number of cophasal slot-vectors.

C. ARRANGEMENT EVALUATION

In this paper, the EMF error between parallel paths is regarded as the basis evaluation for the asymmetric degree of the arrangement. According to the number of cophasal slot-vectors in the path slot-number matrix, the resulting EMF of a parallel path $\dot{E}_j$ can be calculated by:

$$\dot{E}_j = \sum_{k=1}^{q} b_{j,k} \cdot e^{i(k-1)\alpha_1} \tag{5}$$

where i is the imaginary unit, α_1 is the electrical angle of the slot pitch.

The EMF error between parallel paths can be factorized by the magnitude and phase components which can be regarded as two indices for the asymmetric degree. Here, the percentage of EMF error can be calculated by:

$$\Delta = \frac{E_{\max} - E_{\min}}{E_{\max}} \times 100\% \tag{6}$$

where $E_{\max}/E_{\min}$ is the maximum/minimum magnitude of the resulting EMF between parallel paths.

Then, the maximum of EMF phase difference can be written in a form as:

$$\delta = \varphi_{\max} - \varphi_{\min} \tag{7}$$

where $\varphi_{\max}/\varphi_{\min}$ is the maximum/minimum phase of the resulting EMF between parallel paths.

D. CONNECTION FEATURE

As above, the resulting EMF of a parallel path is not changed by exchanging the slot-vector using a cophasal slot-vector. Based on this feature, the cross-pole connection can be avoided by adjusting the combination of cophasal coils. A simple model is provided as an example, and the winding parameters are presented as:

$$\text{Model: } Z = 72, p = 3, a = 4, q = 4 \text{ and } y_1 = 10.$$

where y_1 is the coil pitch.

The square graph of the simple model can be obtained as:

$$\mathbf{N}_{(\text{e.g.})} = \begin{bmatrix} 1 & 2 & 3 & 4 \\ 25 & 26 & 27 & 28 \\ 49 & 50 & 51 & 52 \end{bmatrix}_{3\times4} \quad (8)$$

In addition, the path slot-number matrix of an arrangement can be presented as:

$$\mathbf{B}_{(\text{e.g.})} = \begin{bmatrix} 1 & 2 & 2 & 1 \\ 2 & 1 & 1 & 2 \end{bmatrix}_{2\times4} \quad (9)$$

In Fig. 2(a), (b), a cross-pole connection 2 → 51 exists in parallel path A2. By adjusting the colphasal coils, the cross-pole connection can be removed, as shown in Fig. 2(c), (d). For details, the coil 51 of parallel path A2 is replaced by the colphasal coil 27 of parallel path A1, and the coil 28 of parallel path A2 is replaced by the colphasal coil 52 of parallel path A1. Comparing two connections, the number of the colphasal slot-vectors for each parallel path is not changed. Thus, the asymmetric degree is not changed.

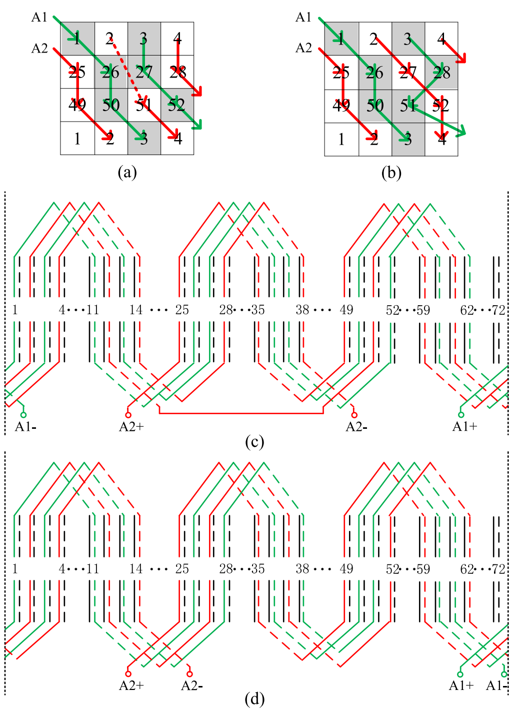

FIGURE 2. Connections of simple model for phase-belt A. (a) Square graph of original connection. (b) Square graph of adjusted connection. (c) Developed diagram of original connection. (d) Developed diagram of adjusted connection.

III. PROPOSED COMBINATORIAL APPROACH

A. ARRANGEMENT RULES

According to the parameter constraints, three rules for the arrangement optimization should be followed.

a) The range for the number of the cophasal slot-vectors of a parallel path is limited to $0 \sim p$.

b) The sum for the number of a kind of cophasal slot-vectors for all parallel paths should equal p.

c) The total number of slot-vectors of a parallel path should be the same, and the value should equal n_1.

By comparing the EMF error between parallel paths among possible combinations of the slot-vectors, the optimized arrangements with a low asymmetric degree can be obtained and stored in the path slot-number matrix.

B. GROUPING RULES

In this paper, some strategies of grouping are adopted to avoid the useless connections when the coils are assigned to all parallel paths simultaneously. It is an effective method to reduce the operation number in the process of the matching. The path slot-number matrix and the square graph should be divided into some groups, and the connections can be obtained by matching operation among the groups above.

Regarding path slot-number matrix, firstly, the elements of two adjacent columns are divided into a group. The group is denoted by the big-group, and it can be defined as:

$$\mathbf{B}_f = \begin{bmatrix} b_{1,2f-1} & \cdots & b_{1,2f} \\ \vdots & \ddots & \vdots \\ b_{a/2,2f-1} & \cdots & b_{a/2,2f} \end{bmatrix} \quad (10)$$

where f is the big-group number, $f = 1, 2, \cdots, q/2$.

In a big-group, according to the row order, each row constitutes a group. The group is denoted by the small-group, and it can be expressed as:

$$\mathbf{B}_{f,d} = \begin{bmatrix} b_{d,2f-1} & \cdots & b_{d,2f} \end{bmatrix} \quad (11)$$

where d is the small-group number, $d = 1, 2, \cdots, a/2$.

The grouping strategy of the square graph is the same as the operation for big-groups. The group is denoted by the square-group, and it can be defined as:

$$\mathbf{N}_f = \begin{bmatrix} n_{1,2f-1} & \cdots & n_{1,2f} \\ \vdots & \ddots & \vdots \\ n_{p,2f-1} & \cdots & n_{p,2f} \end{bmatrix} \quad (12)$$

For example, based on the grouping rules above, two big-groups and four small-groups can be obtained in Fig. 3(a). Similarly, two square-groups are presented in Fig. 3(b).

C. COMBINATON PATTERN OF COILS

In this paper, the combinatorial model for the combination of coils is transformed by the square-group, whose cells should be renumbered by the corresponding row and

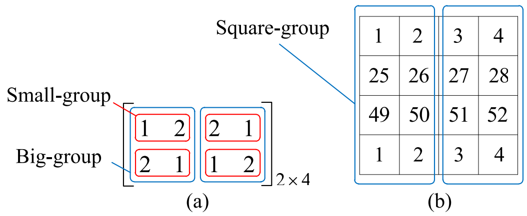

FIGURE 3. Examples for the grouping of simple model. (a) Path slot-number matrix. (b) Square graph.

column numbers, and it can be defined as:

$$\mathbf{N}'_f = \begin{bmatrix} 1_{1,2f-1} & \cdots & 1_{1,2f} \\ \vdots & \ddots & \vdots \\ p_{p,2f-1} & \cdots & p_{p,2f} \end{bmatrix} \tag{13}$$

According to the given total number of coils in the corresponding column of small-group, the combination of the coils can be obtained, and it can be expressed as:

$$\mathbf{C}_{i,j,u_1} = \{c_1, c_2, \cdots, c_g\}_{i,j,u_1} \tag{14}$$

where $c_1, c_2, \cdots, c_g$ are the renumbered coil numbers in the combination of coils, $g = b_{i,j}$, and u_1 is the combination number for corresponding column, $u_1 = 1, 2, \cdots, n^c_{i,j}$.

Here, the number of possible combinations of coils for the corresponding column can be calculated by:

$$n^c_{i,j} = \binom{p}{g} = \frac{p(p-1)\cdots(p-g+1)}{g(g-1)\cdots 1} \tag{15}$$

The steps for the coil combination in a column of a small-group are presented in Alg. 1.

Algorithm 1 Coil Combination in a Column of Small-Group

Input Row vector of all coils in corresponding column (R), given selection number of coils (N)
Output Combinations of coils (C)

```
M ← the number of elements of R;
if M is equal to N then
    C ← R;
else if N is equal to 1 then
    C ← R^T;
else
    C ← Ø;
for k1 = 1: M − N + 1 do
recursion by R(k1 + 1:M) and N-1
    return C1
Middle variable w1 ← number of rows of C1;
Middle variable w2 ← Ø;
for k2 = 1:w1 do
w2(k2) ← r(k1);
end for
Middle variable w3 ← [w2^T, C1];
    Middle variable w4 ← C;
    C ← [w4^T, w3^T]^T;
end for
end if
```

Considering the connection order between coils, the permutation of coils can be expressed as:

$$\mathbf{P}_{i,j,u} = \{c_1, c_2, \cdots, c_g\}_{i,j,u} \tag{16}$$

where u is the permutation number, $u = 1, 2, \cdots, n^p_{i,j}$.

Here, the total number of the permutations of coils can be calculated by:

$$n^p_{i,j} = n^c_{i,j} \cdot g! \tag{17}$$

The steps for the coil permutation in a column of a small-group are presented in Alg. 2.

Algorithm 2 Coil Permutation in a Column of Small-Group

Input Row vector for a combination of the coils (C), position of swap (S, initial value is set to S = 1)
Output Permutations of coils (P)

```
M ← the number of elements of C;
if S is equal to M then
    P ← C;
else
    P ← Ø;
for k1 = S:M do
Middle variable w1 ← R(S);
    C(S) ← C(k1);
    C(k1) ← w1;
recursion by C and S + 1
    return P1
Middle variable w2 ← R(S);
    C(S) ← C(k1);
    C(k1) ← w2;
Middle variable w3 ← P;
    P ← [w3^T, P1^T]^T;
end for
end if
```

For example, the procedure of the transformation for the combinatorial model is shown in Fig. 4(a), (b). Here, the small-group 1 is [1, 2], where the element of the second column is 2. It means that there are two coils in the second column of the combinatorial model belonged to the path A1. For details, there are three possible combinations of coils in Fig. 4(c) and six possible combinations with the connection order in Fig. 4(d).

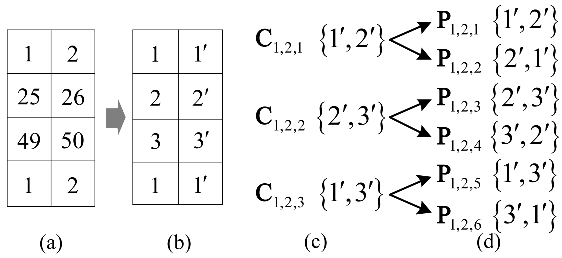

FIGURE 4. Examples for the combination pattern of coils of simple model. (a) Square graph. (b) Combinatorial model. (c) Combinations of coils. (d) Permutations of coils.

D. CONNECTION MATCHING IN A SMALL-GROUP

The effective connections between coils of the small-group can be obtained by matching among possible combinations of coils for each column. According to the connection feature, the connection order is from up to down, and the distance between two adjacent coils is one row.

The matching is carried out by connecting the coils in the possible combinations orderly and testing whether these connections satisfy the connection rules above. During matching, the pointer of the current position for coils of the possible combination in a small-group can be defined as:

$$\mathbf{R}_{f,d} = [r_l]_{f,d} \tag{18}$$

where r_l is position of the coil in corresponding column l.

The steps for the connection matching in a small-group are presented in Alg. 3.

Algorithm 3 Connection Matching in a Small-Group

Input Possible combinations of coils for each column
Output Effective connections of this small-group

```
while k1≠0 do
  Extract a combination of coils for each column;
  All elements of the pointer are initialized by 0;
  Select the first coil in a possible combination of the
  first column, and update the pointer;
  while k2 ≠ 0 do
    The target value ← the row number of the selected
    coil plus 1;
    if the target value is larger than p then
      The target value ← the target value minus p;
    end if
    if the target value equals the row number of any coil
    pointed by current position plus 1 then
      This coil is selected, and test the column number,
      and update the pointer;
      if all elements of pointer reach maximum then
        the matching is successful and the effective connection
        of this small-group should be stored;
        k2 = 0;
      end if
    else
      k2 = 0;
    end if
  end while
  count++;
  if the count reach the maximum then
    k1 = 0;
  end if
end while
```

For example, as above, the combinations of coils for two columns of the small-group 1 are shown in Fig. 5(a). For the matching 1, the pointer is initialized by $[0, 0]$. Select coil 1, and the pointer is updated by $[1, 0]$. The position of the first column reach maximum. Here, the target value is 2. With respect to the first coil of next column, the row number is 1 and not equal to target value. If keep connecting, the cross-pole connection $1 \rightarrow 1'$ appears in Fig. 5(b), and the matching is failed.

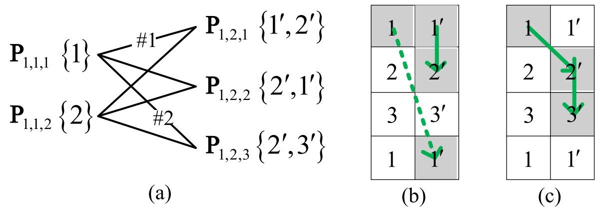

FIGURE 5. Examples for connection matching in the small-group of simple model. (a) Operation procedure. (b) Failed matching. (c) Successful matching.

Similarly, regarding the matching 2, the row number for the first coil of the second column is 2, which is equal to the target value. The coil $2'$ is selected, and the pointer is updated by $[1, 1]$. Then, the second coil $3'$ is selected, and the pointer is $[1, 2]$. All positions reach maximum, and the matching is successful. As shown in Fig. 5(c), the effective connection $1 \rightarrow 2' \rightarrow 3'$ can be obtained.

E. CONNECTION MATCHING IN A BIG-GROUP

The effective connection of the big-group is a part of the phase winding. It can be obtained by the matching among the effective connections of all small-groups in this big-group. The matching is carried out by comparing the union set for the coils of the effective connections with the set for all coils of the corresponding combinatorial model.

The set of coils for an effective connection of a small-group can be formed as:

$$\mathbf{M}_{f,d,v} = \left\{c_1, c_2, \cdots c_{g_1}\right\}_{f,d,v} \tag{19}$$

where $g_1 = b_{d,2f-1} + b_{d,2f}$, and v is the combination number for the effective connections of the corresponding small-group.

The union set for the effective connections of small-groups can be calculated by:

$$U_{f,v} = \bigcup_{d=1}^{a/2} \mathbf{M}_{f,d,v} \tag{20}$$

The steps for the connection matching in a big-group are presented in Alg. 4.

For example, one effective connection of path A1 and two connections of path A2 are presented in Fig. 6(a). With respect to the matching 1, the union set of $\mathbf{M}_{1,1,1}$ and $\mathbf{M}_{1,2,1}$ is $\left\{1, 2', 3', 3\right\}$. In Fig. 6(b), the coils $1'$, 2 are missed, and matching is failed. On the contrary, for the matching 2, the union set of $\mathbf{M}_{1,1,1}$ and $\mathbf{M}_{1,2,2}$ is $\left\{1, 2', 3', 2, 3, 1'\right\}$. All coils are included in Fig. 6(c), and the matching is successful. The effective connection of this big-group can be obtained.

Algorithm 4 Connection Matching in a Big-Group

Input Effective connections for each small-group
Output Effective connections of this big-group

```
while k1≠0 do
  Extract a combination for the effective connection of
   each small-group;
  The union set of coils for the effective connection of
   each path should be calculated by using (20);
  if the union set includes all coils then
    The matching is successful, and the effective
     connection of this big-group should be stored;
  end if
  count++;
  if the count reach the maximum then
    k1 = 0;
  end if
end while
```

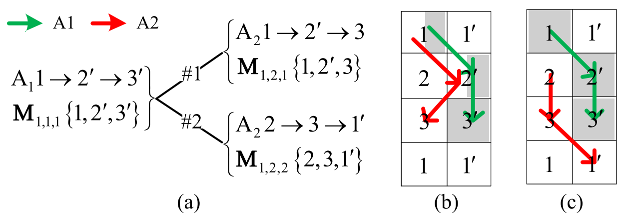

FIGURE 6. Examples for connection matching in the big-group of simple model. (a) Operation procedure. (b) Failed matching. (c) Successful matching.

F. CONNECTION MATCHING BETWEEN BIG-GROUPS

The whole connection can be obtained by the matching between the effective connections of adjacent big-groups. The matching is carried out by testing the difference between the head-data and the tail-data for each parallel path between two adjacent big-groups. The head-data/tail-data is the row number of the start/end coil for an effective connection of a small-group. In addition, if the end coil is located in the bottom row, the tail-data is set to zero.

The head-tail matrix is an expression for the head-data and tail-data of the effective connection of a small-group, and it can be defined as:

$$\mathbf{H}_{f,d,w} = \left[\, h_{f,d,w} \quad t_{f,d,w} \,\right] \tag{21}$$

where w is the combination number for effective connections between two big-groups. $h_{f,d,w}/t_{f,d,w}$ is the corresponding head-data/tail-data.

The difference between head-data and tail-data for the effective connection can be calculated by:

$$D_{f,d,w} = h_{f+1,d,w} - t_{f,d,w} \tag{22}$$

As connection rules, the difference between the tail-data of a parallel path of a big-group and the head-data of the same parallel path of the back big-group should equal to +1.

The steps for the connection matching between big-groups are presented in Alg. 5.

Algorithm 5 Connection Matching Between Big-Groups

Input Effective connections of two adjacent big-groups
Output Effective connections between two big-groups

```
while k1 ≠ 0 do
  Extract a combination of effective connections of
   parallel paths for these two big-groups;
  The head-tail matrix should be extracted, and the
   difference between head-data and tail-data
   for each path should be calculated by using (22);
  if the difference of each path equals to +1 then
    The matching between these two big-groups is
     successful, and the effective connections of these
     two big-groups should be stored;
  end if
  count++;
  if the count reach the maximum then
    k1 = 0;
  end if
end while
```

For example, there are one effective connection for big-group 1 and two connections for big-group 2, in Fig. 7(a). For the matching 1, the head-data of $\mathbf{H}_{2,1,1}$ is 1, and the tail-data of $\mathbf{H}_{1,1,1}$ is 0. The difference between the head-data and tail-data for parallel path A1 is $1 - 0 = 1$. In this way, the difference for parallel path A2 is $3 - 1 = 2$ and not equal to 1. As shown in Fig. 7(b), the cross-pole connection $1' \rightarrow 3$ exists, and matching is failed. With respect to the matching 2, all differences are equal to 1, and matching is successful. The effective connection can be obtained, in Fig. 7(c).

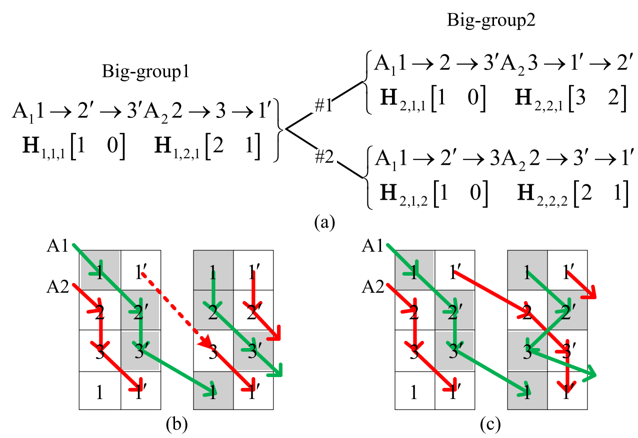

FIGURE 7. Examples for connection matching between big-groups of simple model. (a) Operation procedure. (b) Failed matching. (c) Successful matching.

IV. EXAMPLE ANALYSIS

To validate the feasibility of the proposed approach, the design of the stator winding of a large hydro-generator is provided in this section. Detailed design parameters of the machine are presented in TABLE 1. In addition, the basis parameters of windings are provided as:

Machine: $Z = 252$, $p = 7$, $a = 4$, $q = 6$ and $y_1 = 15$.

TABLE 1. Design parameters of the machine.

Parameter	Value
Rated power	300 MW
Rated voltage	18 kV
Rated current	10691.7 A
Phase resistance	0.001249 Ω
Rotor inner radius	1682 mm
Rotor outer radius	2194 mm
Stator outer radius	3175 mm
Minimum/Maximum air gap	46/62 mm
Core length	3250 mm

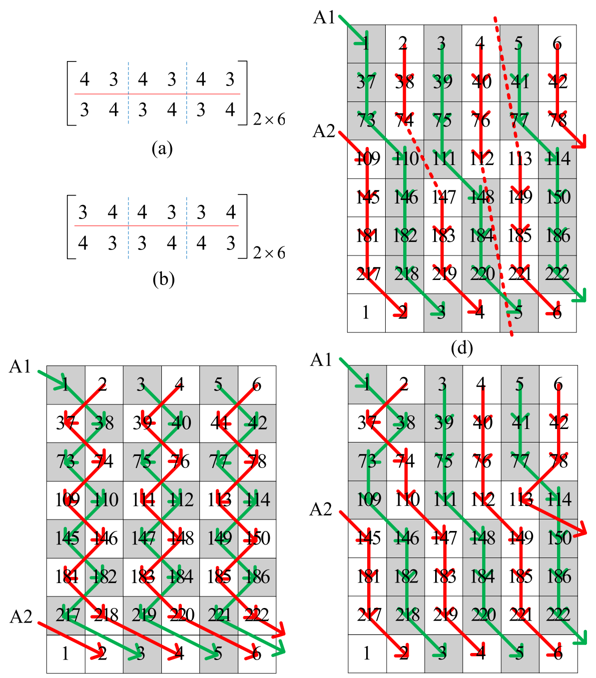

FIGURE 8. Path slot-number matrixes and square graphs for phase-belt A. (a) Existing arrangement. (b) Optimized arrangement. (c) Connection for the existing arrangement. (d) Existing connection for the optimized arrangement. (e) Optimized connection for the optimized arrangement.

According to the winding parameters above, the optimization model can be obtained. Two designs are presented in Fig. 8, where the existing design adopts a constant alternative distribution of coils. With respect to this distribution, the tidiness of end connection can be ensured, as shown in Fig. 8(c), but the asymmetric degree is a bit high. From the results in TABLE 2, the optimized design presents the advantage on the EMF phase difference. Nevertheless, a tidy end connection of this unusual distribution can hardly be obtained by the existing method. As shown in Fig. 8(d), two cross-pole connections 74 → 147 and 112 → 113 exist in parallel path A2. Through adjusting the combination and the connection order of coils, these cross-pole connections can be removed effectively in Fig. 8(e). The developed diagrams for three connections are shown in Fig. 9. The tidiness of end connections for the optimized design can be ensured.

TABLE 2. Calculated results for the asymmetric degree.

Design	Δ (%)	δ (°)
(Exist.)	0	1.432
(Opt.)	1.77e-14	0.437

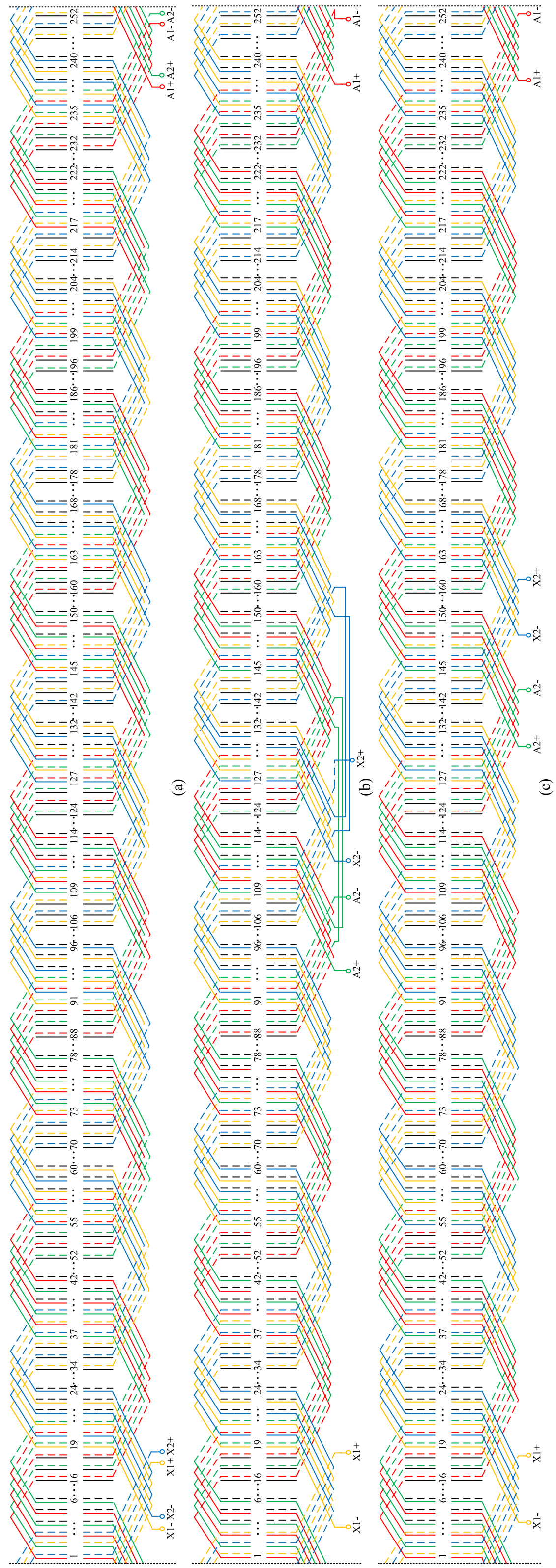

FIGURE 9. Developed diagrams for phase A. (a) Connection for the existing arrangement. (b) Existing connection for the optimized arrangement. (c) Optimized connection for the optimized arrangement.

The analyses in the electromagnetic field are provided as follows. The resulting EMF of each parallel path can be obtained by setting all parallel paths under open circuit condition. The distributions of the resulting EMFs are shown in Fig. 10. Compared with two designs, the differences among the voltage waveforms are small similarly.

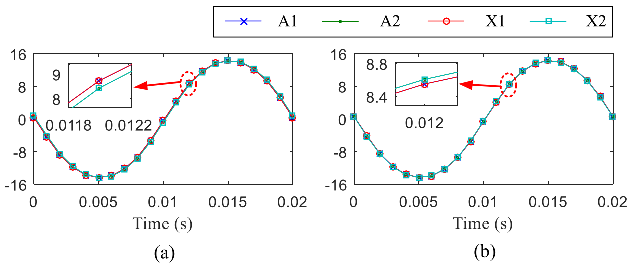

FIGURE 10. Voltage waveforms for parallel paths of phase A (kV). (a) Existing design. (b) Optimized design.

By harmonic analysis, the statistical results for the fundamental component are presented in TABLE 3. The calculated results for parallel path A1 and A2 are almost same as those of parallel path X1 and X2 respectively. By calculation, the $\Delta(\%)$ for the existing/optimized design are $3.06 \times 10^{-5}\%/7.49 \times 10^{-6}\%$, and the $\delta(°)$ for the existing/optimized design are 1.43°/0.44°, which are close to the corresponding presented results of the asymmetric degree.

TABLE 3. Calculated results for path voltages of phase A.

Path	Magnitude component (V)		Phase component (°)	
	(Exist.)	(Opt.)	(Exist.)	(Opt.)
A1	14691.94	14690.75	88.47	87.53
A2	14691.59	14690.71	87.04	87.97
X1	14692.04	14690.78	88.47	87.53
X2	14691.63	14690.82	87.04	87.97

Regarding the distribution of the magnetic field, as shown in Fig. 11, there is no obvious difference between the distributions of the magnetic field line under same working condition. Particularly, because of the armature reaction, the axis of the magnetic field line deviates from the d-axis under rated-load condition, which could bring the harmonic increase in the distribution of flux density in air-gap.

As shown in Fig. 12(a), (c), the overlap ratio between curves is very high under corresponding working conditions. It indicates that the circulating current has little effect on the distribution of magnetic field, owing to the symmetrical distribution between phase windings. Comparing two conditions, the curves under rated-load condition presents higher harmonic content with phase advance than the no-load condition, which is mainly caused by the armature reaction and magnetic saturation.

By harmonic analysis, all harmonic components for two designs are approximately same in Fig. 12(b), (d). Under no-load condition, the amplitude of the fundamental component is about 1T, and the harmonic distortions for 3th, 5th, 7th, and 9th are under 4.9%, 3.4%, 3.7%, and 1.9%. Under rated-load condition, the amplitude of the fundamental component is 1.1T approximately, and other harmonic distortions are about 12.8%, 3.8%, 3.5%, 2.1% respectively. The amplitude of the 3th harmonic component increases obviously.

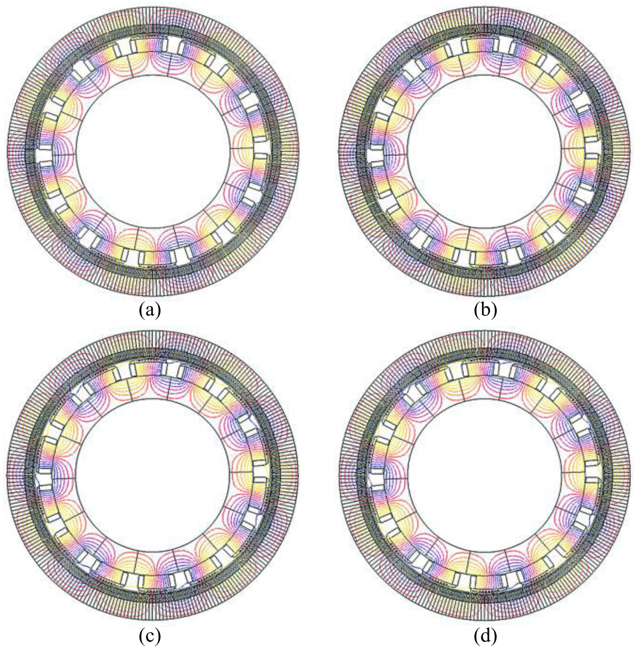

FIGURE 11. Trajectories of the magnetic field for two designs. (a) Existing design under no-load condition. (b) Optimized design under no-load condition. (c) Existing design under rated-load condition. (d) Optimized design under rated-load condition.

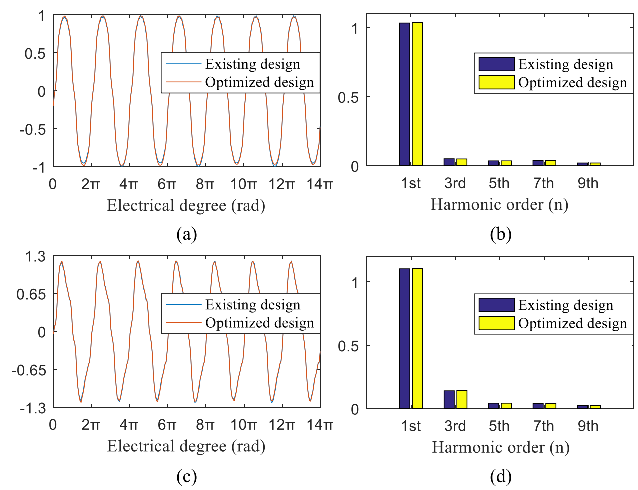

FIGURE 12. Comparisons for the flux density in air-gap (T). (a) Distribution of flux density under no-load condition. (b) Harmonic analysis under no-load condition. (c) Distribution of flux density under rated-load condition. (d) Harmonic analysis under rated-load condition.

The distributions of parallel paths are shown in Fig. 13. It can be clearly seen that the differences between paths for the optimized design are much smaller than the existing one which is shown in Fig. 13(a), (c). The statistical results are presented in TABLE 4. With respect to the difference between

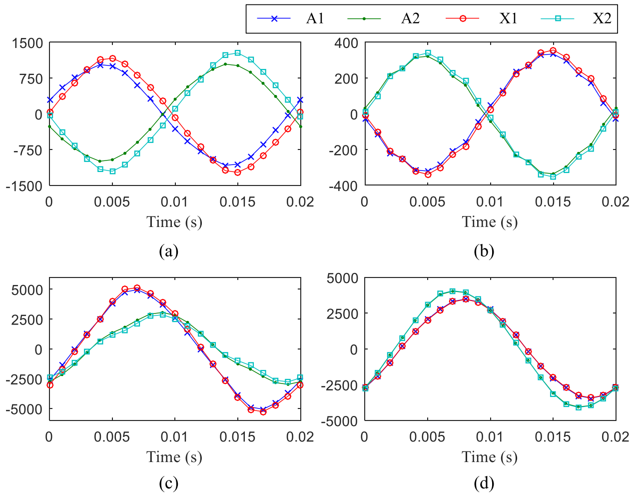

FIGURE 13. Current waveforms for parallel paths of phase A (A). (a) Existing design under no-load condition. (b) Optimized design under no-load condition. (c) Existing design under rated-load condition. (d) Optimized design under rated-load condition.

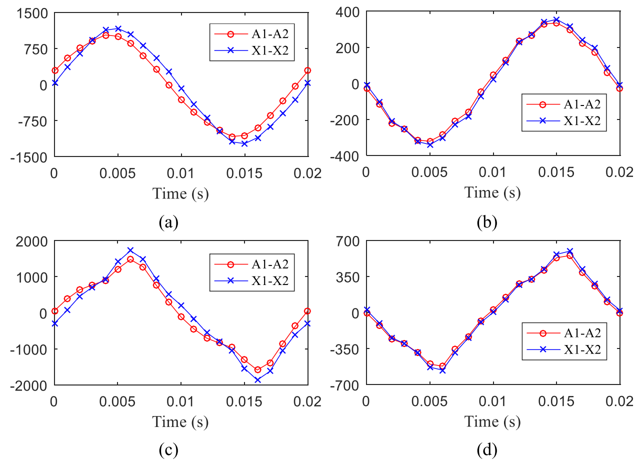

FIGURE 14. Circulating current between parallel paths for phase A (A). (a) Existing design under no-load condition. (b) Optimized design under no-load condition. (c) Existing design under rated-load condition. (d) Optimized design under rated-load condition.

TABLE 4. Calculated results for the path currents of phase A.

Path number	Root-mean-square value (RMS) (A)			
	No-load condition		Rated-load condition	
	(Exist.)	(Opt.)	(Exist.)	(Opt.)
A1	730.67	225.25	3377.00	2185.70
A2	708.00	225.45	2063.48	2584.71
X1	812.38	234.78	3548.17	2164.73
X2	833.00	234.59	1853.29	2606.07

TABLE 5. Calculated results for circulating current and total copper loss of circulating current between parallel paths of phase A.

Condition	Design	RMS of circulating current (A)		Total copper loss of circulating current (W)
		A1-A2	X1-X2	
No-load	(Exist.)	719.31	822.66	11932.2
	(Opt.)	225.35	234.69	1057.8
Rated-load	(Exist.)	931.13	1051.88	19718.8
	(Opt.)	333.57	349.82	2334.6

two path currents, the ratios of existing design to optimized one are 1.03/1.38 for phase-belt A and 1.02/1.59 for phase-belt X under no-load/rated-load condition. Particularly, as shown in Fig. 13(b), the curves of all paths are reversal compared with Fig. 13(a). It means that the resulting EMF of path A2/X2 is ahead of the EMF of path A1/X1. Similarly, as shown in Fig. 13(d), same trend for path current is presented under rated-load condition.

The circulating current between parallel paths can be separated from the path currents. It can be expressed by the average value of the difference between two parallel paths in the same phase-belt. As shown in Fig. 14, compared with the existing design, the curve of the optimized design is reversed. In addition, the harmonic content for rated-load condition is higher than the no-load one. These trends are consistent with the analysis above. The statistical results are presented in TABLE 5. The value of the circulating current for the existing design is about 3.2/2.8 times for phase-belt A/X under no-load condition and about 3.5/3 times for phase-belt A/X under rated-load condition that of the optimized design. With respect to the total copper loss of circulating current, the value of existing design is about 11.3/8.4 times than the optimized one under no-load/rated-load condition. The optimized design presents advantages on the performance in the electromagnetic field.

V. CONCLUSION

In this paper, a novel combinatorial approach is proposed for the modeling and optimization design of the asymmetric-paths winding. It provides a novel direction for the winding design in the perspective of combinatorial mathematics. Through adopting strategies of the grouping in the path slot-number matrix, the square graph and of the matching in corresponding groups, the optimized connection can be obtained from multiple possible schemes.

From validation part, the existing design presents a tidy connection but higher circulating current and total copper loss of circulating current. With respect to the optimized arrangement, the smaller asymmetric degree can be ensured, but the tidiness of end connections can be obtained by the existing method with difficulty. The optimized design presents a smaller asymmetric degree and a tidy connection without cross-pole connections simultaneously. The design contradiction above can be solved effectively. Thus, the efficiency and stability of the machine can be ensured. This approach would be a technical support, in particular, for the optimization design of the asymmetric-paths windings.

REFERENCES

[1] G.-A. Capolino and A. Cavagnino, "New trends in electrical machines technology—Part I," *IEEE Trans. Ind. Electron.*, vol. 61, no. 8, pp. 4281–4285, Aug. 2014.

[2] X. Sun, Y. Shen, S. Wang, G. Lei, Z. Yang, and S. Han, ''Core losses analysis of a novel 16/10 segmented rotor switched reluctance BSG motor for HEVs using nonlinear lumped parameter equivalent circuit model,'' *IEEE/ASME Trans. Mechatronics*, vol. 23, no. 2, pp. 747–757, Apr. 2018.
[3] W. Fong, ''Polyphase windings with multiparallel circuits,'' *Proc. IEE*, vol. 117, no. 10, pp. 1960–1968, Oct. 1970.
[4] Y. C. Zhu, ''Primary study on employing the asymmetric stator windings in hydro-generators,'' *Large Electr. Mach. Hydraulic Turbine*, vol. 18, no. 4, pp. 7–10, 1988.
[5] L. H. Li, Y. P. Liang, and H. Huang, ''Discussion on asymmetric-branches connection of hydro-generator stator winding,'' *Large Electr. Mach. Hydraulic Turbine*, vol. 36, no. 2, pp. 19–22, 2006.
[6] J. X. Li, C. H. Bi, G. Hu, G. F. Li, Y. T. Sun, P. A. Liu, Q. W. Luan, and M. H. Song, ''252-slot and 14-pole asymmetric four-branch two-layer three-phase stator winding,'' China Patent 2011 13 70 696, Nov. 21, 2011.
[7] Y. P. Liang, H. H. Yu, X. Bian, L. L. Gao, and L. Wu, ''Double-deck alternating-current winding of asymmetric integer groove three-phase of four branch roads,'' China Patent 2015 2 197 112 U, Apr. 3, 2015.
[8] Z. Q. Guo, Y. P. Liang, X. Bian, and D. M. Wang, ''Multi-objective optimization for arrangement of the asymmetric-paths winding based on improved discrete particle swarm approach,'' *IEEE Trans. Energy Convers.*, vol. 33, no. 3, pp. 1571–1578, Sep. 2018.
[9] D. G. Dorrell and M. Popescu, ''Effect of winding asymmetries and winding connection on small synchronous machines,'' *IEEE Trans. Ind. Appl.*, vol. 47, no. 6, pp. 2453–2459, Nov./Dec. 2011.
[10] A. O. Di Tommaso, F. Genduso, and R. Miceli, ''A new software tool for design, optimization, and complete analysis of rotating electrical machines windings,'' *IEEE Trans. Magn.*, vol. 51, no. 4, Apr. 2015, Art. no. 9401410.
[11] C. Di, I. Petrov, and J. J. Pyrhönen, ''Design of a high-speed solid-rotor induction machine with an asymmetric winding and suppression of the current unbalance by special coil arrangements,'' *IEEE Access*, vol. 7, pp. 83175–83186, 2019.
[12] Y. P. Liang, Z. Q. Guo, D. M. Wang, and X. Bian, ''Novel directed graph approach for connection optimization of the asymmetric-paths winding,'' *IEEE Trans. Energy Convers.*, to be published. doi: 10.1109/TEC.2019.2930617.
[13] F. J. T. E. Ferreira, M. V. Cistelecan, and A. T. de Almeida, ''Comparison of different tapped windings for flux adjustment in induction motors,'' *IEEE Trans. Energy Convers.*, vol. 29, no. 2, pp. 375–391, Jun. 2014.
[14] A. S. Abdel-Khalik, M. A. Elgenedy, S. Ahmed, and A. M. Massoud, ''An improved fault-tolerant five-phase induction machine using a combined star/pentagon single layer stator winding connection,'' *IEEE Trans. Ind. Electron.*, vol. 63, no. 1, pp. 618–628, Jan. 2016.
[15] S. M. Raziee, O. Misir, and B. Ponick, ''Combined star-delta winding analysis,'' *IEEE Trans. Energy Convers.*, vol. 33, no. 1, pp. 383–394, Mar. 2018.
[16] X. Deng, B. Mecrow, R. Martin, and S. Gadoue, ''Effects of winding connection on performance of a six-phase switched reluctance machine,'' *IEEE Trans. Energy Convers.*, vol. 33, no. 1, pp. 166–178, Mar. 2018.
[17] S. Han, C. Liu, X. Sun, K. Diao, and J. Wu, ''Investigation of static characteristics in six-phase switched reluctance motors under different winding connections,'' *IEEE Access*, vol. 7, pp. 71174–71184, 2019.
[18] L. Chunyan and K. Baoquan, ''Research on electromagnetic force of large thrust force PMLSM used in space electromagnetic launcher,'' *IEEE Trans. Plasma Sci.*, vol. 41, no. 5, pp. 1209–1213, May 2013.
[19] J. Ma, R. Qu, J. Li, and S. Jia, ''Structural optimization of a permanent-magnet direct-drive generator considering eccentric electromagnetic force,'' *IEEE Trans. Magn.*, vol. 51, no. 3, Mar. 2015, Art. no. 8100904.
[20] X. Sun, B. Su, S. Wang, Z. Yang, G. Lei, J. Zhu, and Y. Guo, ''Performance analysis of suspension force and torque in an IBPMSM with V-shaped PMs for flywheel batteries,'' *IEEE Trans. Magn.*, vol. 54, no. 11, Nov. 2018, Art. no. 8105504.
[21] Z. Shi, X. Sun, Y. Cai, Z. Yang, G. Lei, Y. Guo, and J. Zhu, ''Torque analysis and dynamic performance improvement of a PMSM for EVs by skew angle optimization,'' *IEEE Trans. Appl. Supercond.*, vol. 29, no. 2, Mar. 2019, Art. no. 0600305.
[22] X. Sun, K. Diao, G. Lei, Y. Guo, and J. Zhu, ''Study on segmented-rotor switched reluctance motors with different rotor pole numbers for BSG system of hybrid electric vehicles,'' *IEEE Trans. Veh. Technol.*, vol. 68, no. 6, pp. 5537–5547, Jun. 2019.
[23] M. Dorigo, V. Maniezzo, and A. Colorni, ''Ant system: Optimization by a colony of cooperating agents,'' *IEEE Trans. Syst., Man, Cybern. B, Cybern.*, vol. 26, no. 1, pp. 29–41, Feb. 1996.
[24] M. Dorigo and L. M. Gambardella, ''Ant colony system: A cooperative learning approach to the traveling salesman problem,'' *IEEE Trans. Evol. Comput.*, vol. 1, no. 1, pp. 53–66, Apr. 1997.
[25] A. Khodaei and M. Shahidehpour, ''Microgrid-based co-optimization of generation and transmission planning in power systems,'' *IEEE Trans. Power Syst.*, vol. 28, no. 2, pp. 1582–1590, May 2013.
[26] A. Canova, F. Freschi, and M. Tartaglia, ''Multiobjective optimization of parallel cable layout,'' *IEEE Trans. Magn.*, vol. 43, no. 10, pp. 3914–3920, Oct. 2007.
[27] E. Plaku, L. E. Kavraki, and M. Y. Vardi, ''Motion planning with dynamics by a synergistic combination of layers of planning,'' *IEEE Trans. Robot.*, vol. 26, no. 3, pp. 469–482, Jun. 2010.
[28] G. Hong, T. Wei, and X. Ding, ''Multi-objective optimal design of permanent magnet synchronous motor for high efficiency and high dynamic performance,'' *IEEE Access*, vol. 6, pp. 23568–23581, 2018.
[29] Y. Du, W. Lu, X. Zhu, and L. Quan, ''Optimal design and analysis of partitioned stator hybrid excitation doubly salient machine,'' *IEEE Access*, vol. 6, pp. 57700–57707, 2018.
[30] X. Cui, J. Sun, C. Gan, C. Gu, and Z. Zhang, ''Optimal design of saturated switched reluctance machine for low speed electric vehicles by subset quasi-orthogonal algorithm,'' *IEEE Access*, vol. 7, pp. 101086–101095, 2019. doi: 10.1109/ACCESS.2019.2929103.

YANPING LIANG was born in Harbin, China, in 1963. She received the M.S. degree in electrical machines from the Harbin University of Science and Technology, Harbin, in 1988, and the Ph.D. degree in electrical machines from the Harbin Institute of Technology, Harbin, in 2005.

She is currently a Professor with the Harbin University of Science and Technology. Her research interests include electrical machine electromagnetic theory and design, large generator electromechanical energy conversion, and electromagnetic field calculation.

Dr. Liang is a Senior Member of the China Electrotechnical Society.

ZHONGQI GUO was born in Hulunbuir, China, in 1992. He received the B.S. degree from Inner Mongolia Agricultural University, Hohhot, China, in 2013. He is currently pursuing the Ph.D. degree in electrical engineering with the Harbin University of Science and Technology.

His research interests focus on the winding design, simulating calculation, and optimization method.

XU BIAN was born in Harbin, China, in 1988. She received the B.S., M.S., and Ph.D. degrees in electrical machines from the Harbin University of Science and Technology, Harbin, in 2010, 2013, and 2016, respectively.

She is currently an Associate Professor with the Harbin University of Science and Technology. Her research interests include electromagnetics, fluid and thermal analysis, and design of large electrical machines.

CHENGUANG WANG was born in Xingtai, China, in 1984. He received the B.S. and M.S. degrees in signal and information processing from the Harbin University of Science and Technology, Harbin, China, in 2005 and 2008, respectively, where he is currently pursuing the Ph.D. degree in electrical machines.

He is also a Lecturer with the Harbin University of Science and Technology. His research interests include electromagnetic calculation, electromagnetic measurement technology, and stator windings fault diagnosis.

DONGMEI WANG was born in Mudanjiang, China, in 1989. She received the B.S. and M.S. degrees from the Harbin University of Science and Technology, Harbin, China, in 2012 and 2015, respectively, where she is currently pursuing the Ph.D. degree in electrical machines.

She is currently a Lecturer with the Harbin University of Science and Technology. Her research interests include the electromagnetic, and fluid and thermal analysis on electrical machines.

LIANLIAN GAO was born in Yichun, China, in 1990. She received the B.S. and Ph.D. degrees in electrical machines from the Harbin Institute of Electrical Technology, Harbin, China, in 2012 and 2018, respectively.

She is currently a Lecturer with the Harbin University of Science and Technology. Her research interests include research on electromagnetic and operation analysis on electromagnetic equipment.